ELSEVIER

International Journal of Heat and Fluid Flow 22 (2001) 509–518

International Journal of HEAT AND FLUID FLOW

www.elsevier.com/locate/ijhff

Heat-transfer enhancement in a channel flow with perforated rectangular blocks

O.N. Sara [a], T. Pekdemir [b,*], S. Yapici [a], M. Yilmaz [a]

[a] *Faculty of Engineering, Atatürk University, 25240 Erzurum, Turkey*

[b] *Department of Mechanical and Chemical Engineering, Heriot-Watt University, Edinburgh EH14 4A5, UK*

Received 24 June 2000; accepted 3 June 2001

Abstract

The present paper reports heat-transfer enhancement and the corresponding pressure drop over a flat surface in a channel flow due to perforated rectangular cross-sectional blocks attached on its surface. The channel had a cross-sectional area of 80×160 mm^2 with blocks 10×25 mm^2. The experiments covered the following range: Reynolds number (Re) 6670–40 000, the hole inclination angle (θ) 0–45°, the perforation open-area ratio (ϕ) 0.05–0.15, the diameter of the perforations (D) 2.5–8.0 mm, and the number of the blocks (N_b) 2–7 (giving the ratio of the distance between the blocks to the channel hydraulic diameter (S_x/D_e) 1.407–0.309). The blocks were transverse to the main flow. It was observed that the heat-transfer enhancement increased with increasing θ, ϕ and D and decreasing S_x/D_e and Re. The pressure drop was not affected by θ while it decreased with increasing D, Re, S_x/D_e, and ϕ. Correlation equations were developed for the average Nusselt number ($\overline{Nu}$) and the friction factor (f). Performance analysis indicated that the solid blocks could lead to energy loses up to 20% despite significantly enhanced heat-transfer due to the increased surface area. The energy lost was recovered by perforations opened in the blocks by which means it was possible to achieve energy gains up to 40%.

Keywords: Heat-transfer enhancement; Channel flow; Rectangular blocks; Perforated blocks; Forced convection; Heat exchangers

1. Introduction

The increasing necessity for saving energy and material imposed by the diminishing world resources and environmental concerns have prompted the development of more effective heat-transfer equipment with improved heat-transfer rates. In many industrial systems, heat must be transferred either to input energy into the system or to remove the energy produced in the system. Considering the rapid increase in energy demand world-wide, both reducing energy lost due to ineffective use and enhancement of the energy transfer in the form of heat have become an increasingly important task for the design and operation engineers for such systems.

In recent years, many techniques have been proposed for the enhancement of the heat-transfer rate. These can be classified into two main groups: (i) passive techniques not requiring additional power sources, (ii) active techniques requiring additional external power inputs (Bergles and Webb, 1985; Reay, 1991). In the case of passive techniques, convection heat transfer from surfaces with attachments of different solid shapes with different geometry, such as fins, ribs, blocks, have been widely exploited (Ledezma et al., 1996; Goldstein et al., 1994; Tahat et al., 1994; Jurban et al., 1993; Babus'Haq et al., 1993; Naik et al., 1987; Liou and Hwang, 1992, 1993; Hong and Hsieh (1993); Hwang and Liou, 1994; Hwang and Liou, 1995a,b; Liou et al., 1995; Han, 1988; Zhang et al., 1994; Molki and Mostoufizadeh, 1989; Molki et al., 1995). Heat-transfer enhancement with such arrangements is achieved by the increase in the surface area (surface extension) and also by the turbulence (mixing) generated due the attachments. This type of forced convection heat transfer is encountered in much process equipment such as heat exchangers, nuclear reactor fuel elements, turbine blades, electronic boards and components etc. Improved heat-transfer rates are normally accompanied by increases in the pressure drop in the flow over such surfaces. Thus the main target is to design the attachments in such a way and geometry that they will yield maximum enhancement in the heat-transfer rate with minimum increase in the pressure drop or minimum decrease in the flow rate.

Our earlier studies (Sara, 1998; Sara et al., 2001) as well as those by Hwang and Liou (1994, 1995a,b) showed that when solid blocks are positioned with an angle of attack of 90° to the main (bulk) flow direction (transverse positioning), hot zones develop in the wake of the blocks because of the low speed recirculating flow in the region. This results in lower heat-

* Corresponding author. Tel.: +44-131-451-8145; fax: +44-131-451-3129.

E-mail address: t.pekdemir@hw.ac.uk (T. Pekdemir).

0142-727X/01/$ - see front matter
PII: S0142-727X(01)00117-5

Notation

A	heat-transfer area
C	clearance between the upper surface of the blocks and ceiling of the duct
D	perforation hole diameter
D_e	hydraulic diameter of the channel
f	friction factor
H	height of the blocks
$\overline{h}$	average convective heat-transfer coefficient
k_{air}	thermal conductivity of air
L	length of test surface
L_t	length of test section
N	number of the holes in a block
N_b	number of the blocks
$\overline{Nu}$	average Nusselt number for the blocked surface
$\overline{Nu}_s$	average Nusselt number for the smooth surface
$\overline{Nu}_s^*$	average Nusselt number for the smooth surface with Re_s at which the pumping power is the same as that occurring in the blocked surface
Pr	Prandtl number
Q	heat-transfer rate
Re	Reynolds number ($=uD_e\rho\mu$)
S_x	distance between back surfaces of two consecutive blocks in x direction
$\overline{T}$	mean temperature
t	thickness of the blocks
u	mean bulk flow velocity
W	width of the base plate or length of the blocks
ΔP	pressure drop
μ	air viscosity
θ	angle between the axis of the holes and the horizontal axis of the channel
ρ	air density
ϕ	perforated blocks open-area ratio

Subscripts

b	blocks
c	calculated
conv	convective
e	experimental
elect	electrical
in	conditions at the inlet
loss	loss
out	conditions at the outlet
s	smooth
w	conditions at the surface

transfer rates from the-surface. The severity of this adverse effect may change significantly depending on the flow and geometrical conditions. There have been attempts to overcome this adverse effect by different design of the blocks. Our previous study (Sara et al., 2001) and that of Lau et al. (1991) showed that as the angle of attack decreases the adverse effects diminish and beyond a certain point, depending again on the flow and the geometrical conditions, the heat-transfer rate is enhanced.

Another way of improving the heat-transfer characteristics is to employ attachments with (i) perforations (Tanasawa et al., 1983; Yamada and Osaka, 1992; Hwang and Liou, 1994, 1995a,b; Liou and Chen, 1998), (ii) a certain degree of porosity (Ichimaya et al., 1991), or (iii) slots (Tanasawa et al., 1983 and Hwang, 1998) which allow the flow to go through the blocks. The above studies and the work of Liou et al. (1998), investigating the effect of perforated ribs on the flow field in a rectangular duct, reported that the surfaces with permeable attachments resulted in reducing the hot zone regions (extent of the separated flow region) that usually occurred mainly behind and, up to a certain size, in front of their solid counterparts and thus led to significant heat-transfer enhancement. However, the existence of flow passages in the blocks does not always mean that the blocks are "flow permeable". There appears to be a permeability limit which is a function only of the block open-area ratio and the main flow Reynolds number, but not influenced by block spacing and height (Hwang and Liou, 1994). The criterion for the blocks to be considered as permeable is the occurrence of a change in the flow pattern. According to Hwang and Liou (1994), when the blocks are permeable, a mixing layer flow pattern appears behind the blocks.

In the case of perforated attachments, the improvement in the flow (thus the enhancement in the heat transfer) is brought about by the multiple jet-like flows through the perforations (Liou et al., 1998). Jet flows are associated with high overall and localised transport characteristics (Pekdemir, 1994) not only due to increased shear-induced mixing (turbulence) at the edges of the jet as flow progress downstream but also to high velocities and turbulence (depending on the distance from the jet exit) in the impact zone. It has also been reported in the same study that the impact angle affects transport characteristics of the jet flow significantly and that the more perpendicular the jet to the target surface the higher the transport properties of the flow. But the perforations used in previous studies were all parallel to the base plate surface and, hence, the improvement in the flow they caused were only by the mixing generated due to the jet-like flows trough the holes. In the present work we intend to improve the flow conditions further by directing the flow trough inclined perforations more towards the base plate surface, thus obtaining higher heat-transfer rates. Due to the geometrical constraints of the present experimental set-up, we were able to investigate the effect of the inclination angle only up to 45°.

As mentioned earlier, the heat-transfer enhancement is achieved at the expense of an increased pressure drop. Energy lost due to the pressure drop may sometimes exceed that gained due to the heat-transfer enhancement. For many practical applications, it may thus be necessary to determine the net economic benefit due to the heat-transfer enhancement. Thus, this study has aimed to determine the effect of the blocks on the overall energy performance of the present heat-transfer system by a thermal performance analysis, considering simultaneously measured pressure drops over the test section.

2. Experimental details

The channel flow experimental rig is shown in Fig. 1(a). The rig consisted of a closed rectangular channel with a removable test section (7) and two fans (6 and 9), a data acquisition system (11), an inclined manometer (12), an anemometer/thermometer (2), and a number of thermocouples (8).

The channel, constructed of wood of 20 mm thickness, had an internal cross-section of 160 mm width and 80 mm height (channel aspect ratio 2:1, hydraulic diameter, $D_e = 106.7$ mm). The total length of the channel was 2000 mm. It was operated in suction mode and positioned horizontally. A flow straightener (1) was fitted immediately after the inlet to the channel.

The test section (7), of which only the bottom surface was heated (Fig. 1(b)), was located 900 mm downstream of the flow straightener. The upper wall of the test section was fitted with a glass window which enabled visual observation of the

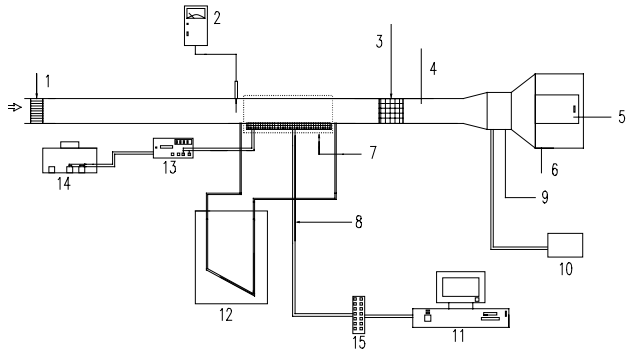

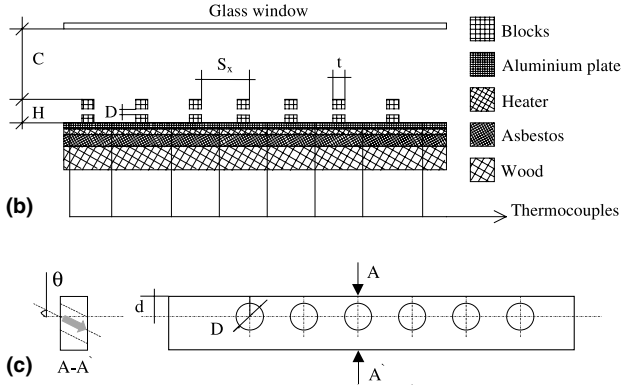

Fig. 1. (a) A schematic display of the experimental set-up, (b) a detailed sketch of the test section with blocks of straight perforations, and (c) a sketch of a block with inclined perforations.

test surface and also permitted alteration on the surface for different arrangements of the blocks to be made when necessary. A flow mixer (3) was fitted 100 mm downstream of the heated surface for homogenising the heated air prior to the mean outlet temperature measurement (4). The base plate of the test surface was made of a smooth aluminium plate of 2 mm thickness, 140 mm width, and 320 mm length. An electrical heater (or thermofoil) with the same dimensions of the base plate was fitted immediately underneath the plate. A thin layer of thermal glue with negligible heat resistance was applied between the heater and the plate to provide a complete contact. In order to minimise the heat loss the other surfaces of the heater were insulated by a combination of a 12 mm thick asbestos layer and a 20 mm thick wood layer. With the present arrangements, it was possible to apply an electrical heat up to 808 Wm^{-2} to the base plate. Current and voltage measurements were performed with an ADM-21162 multimeter (13).

Blocks with a rectangular cross-section of 25 mm height and 10 mm width (i.e., thickness), and a length of 140 mm were attached only on the upper surface of the base plate (Fig. 1(a) and (b)). Thus the ratio of the height of the blocks to the clearance between the upper surface of the blocks and the ceiling of the channel (H/C) was fixed at a value of 0.454. The thermal glue was also applied between the plate and the blocks for better contact. The blocks were made of the same aluminium material as the base plate because of the considerations of conductivity, machinability and cost. They were aligned to the main flow at an angle of attack of 90° (i.e., transverse to the flow). As shown in Fig. 1(b) and (c), the parameters pertinent to the block geometry investigated were, the diameter of the perforations, $D = 2.5$, 4.5 and 8 mm, the perforation inclination angle, $\theta = 0°$, 15°, 30° and 45°, the number of the blocks (i.e., spacing), $N_b = 2$, 3, 4 and 7 (giving values of the ratio of the distance between the blocks (block pitch) to channel hydraulic diameter, $S_x/D_e = 1.407$, 1.116, 0.713 and 0.309). The open-area ratio of the perforated blocks was defined as:

$$\phi = \frac{\text{Sum of the surface areas of the pieces removed to make perforations in a single block}}{\text{Surface area of a single solid block}} = \frac{N\left(2\frac{\pi D^2}{4} + \pi D t\right)}{2(Ht + Wt + HW)}, \quad (1)$$

where t is the width, W the length (also the width of the base plate) and H the height of the block, and N the number of holes in a block. The different values of ϕ were obtained mostly by changing N and keeping N_b and D constant at 4 and 4.5 mm, respectively. N changed in such a way that it gave perforation values, $\phi = 0.05$, 0.10 and 0.15. A few different values of ϕ were obtained by changing D and keeping N_b and N constant for the same ϕ values as above to investigate influence of D and N on the effect of ϕ.

Eight thermocouples of K-type were fitted on the central axis line of the base plate flush with its outer surface for the measurement of the local surface temperatures (Fig. 1(b)). The thermocouples were equi-spaced and, in all cases, positioned in the spaces between the blocks. As the aim was to measure the steady-state average heat-transfer rate from the test surface, it was assumed that the average of temperature readings from eight thermocouples would represent the actual average surface temperature with a good degree of accuracy. Moreover, the heat-transfer enhancement performance due to the perforated blocks was evaluated in comparison to that of the solid blocks (without perforation) so that any error involved due to this assumption will be obviated. Therefore, to simplify the experimental set-up there was no thermocouple attached to the blocks. The temperature readings from the eight thermocouples and from those at the inlet and outlet were all recorded after reaching steady-state conditions by using a PC (11) equipped with an external Advantech PCCD-8115 terminal board (15) and an internal Advantech 818HG data acquisition card (11). Another thermocouple of the same type was used to measure the temperature of the outer surface of the bottom wall of the test section. Readings from this thermocouple were also recorded in steady-state conditions by using the same data acquisition system and these were used in the evaluation of the conductive heat loss from the bottom surface of the test section.

The pressure drop across the test section under heated conditions was determined using pressure taps and an inclined glass tube kerosene manometer (12).

The mean air velocity over the test surface (bulk mean velocity, u) was determined by averaging the local measurements across the channel cross-section using an electronic thermal anemometer (2) of type Airflow TA2-15/3k with a slim probe operating on hot-wire velocity measurement principles. The uncertainty involved in the velocity readings was ±2%. The flow conditions were characterised in terms of Reynolds number (Re), which was based on the hydraulic diameter of the channel over the test section (D_e) and u. Re changed in the range 6670–40 000. The experimental heat-transfer system had a Prandtl number (Pr) of ~0.7.

3. Data reduction

The steady-state energy balance for the electrically heated test surface may be given as:

$$Q_{\text{elect}} = Q_{\text{conv}} + Q_{\text{loss}}, \tag{2}$$

where Q indicates the heat-transfer rate and subscripts elect, conv, and loss donate electrical, convection, and loss, respectively. The electrical heat input is calculated from the electrical potential and current supplied to the surface.

Heat loss from the system may be by (i) radiation from the surface and (ii) conduction through the walls of the channel to the atmosphere. In similar studies, Naik et al. (1987) and Hwang and Liou (1995b) reported that the total radiative heat loss from a similar test surface would be about 0.5% of the total electrical heat input. Therefore, the radiative heat loss was neglected. The conductive heat loss from the side walls can be neglected in comparison to that from the bottom surface of the test section since the total side areas of the heated plate ($2 \times (2 \times 320) = 1280$ cm^2) is only 2.8% of that of the bottom surface ($140 \times 320 = 44\,800$ cm^2). Moreover, as mentioned above, those surfaces of the test plate which were not exposed to the flow had been insulated by a combination of a 12 mm thick asbestos layer and a 20 mm thick wood layer. Thus, it is thought that the conductive heat loss from the heated plate will be mainly from its back surface into the environment through the bottom wall of the channel. This was evaluated for steady-state conditions by using experimentally measured mean temperature of the outer surface of the bottom wall of the test section and a well tried correlation equation suggested for natural convection for geometrically similar systems (Incropera and Dewitt, 1996). The results indicated that, for the extreme conditions, the maximum loss was 7% of the total electrical heat supplied to the surface. This conductive heat loss from the bottom surface was taken into the account in the calculations of the average heat-transfer coefficient of the test surface.

The steady-state convection heat-transfer rate from the test surface can be given by (Naik et al., 1987)

$$Q_{\text{conv}} = \overline{h}A\left[\overline{T}_{\text{w}} - \left(\frac{\overline{T}_{\text{out}} + \overline{T}_{\text{in}}}{2}\right)\right], \tag{3}$$

where $\overline{h}$ is the average convective heat-transfer coefficient, $\overline{T}_{\text{w}}$ the average surface temperature, $\overline{T}_{\text{out}}$ and $\overline{T}_{\text{in}}$ mean temperature of the flow at the outlet and the inlet, respectively, and A the surface area. Either the projected area (A_{P}) or the total area (A_{T}) of the test surface can be taken as the heat-transfer surface area in the calculations. These two areas are related to each other by

$$\begin{aligned} &\text{Total area} = \text{Projected area} + \text{Total surface area} \\ &\qquad\qquad \text{contribution from the blocks:} \\ &A_{\text{T}} = WL + 2N_{\text{b}}[(HW + Ht) \\ &\qquad + \pi N(0.5Dt - 0.25D^2)], \end{aligned} \tag{4}$$

where L is the length of the base plate. It should be noted that the second term in the square brackets represents the area contributions due to the perforation. This term should be omitted when calculating the surface area contribution due to the solid blocks. The average convective heat-transfer coefficient can thus be calculated by

$$\overline{h} = \frac{Q_{\text{elect}} - Q_{\text{loss}}}{A\left[\overline{T}_{\text{w}} - \left(\frac{\overline{T}_{\text{out}} + \overline{T}_{\text{in}}}{2}\right)\right]}. \tag{5}$$

The average convection heat-transfer coefficient may also be presented in terms of average Nusselt number ($\overline{Nu}$) which can be evaluated from

$$\overline{Nu} = \frac{\overline{h}D_{\text{e}}}{k_{\text{air}}}, \tag{6}$$

where k_{air} is the thermal conductivity of air. $\overline{Nu}$ can be calculated on the basis of both the total area and the projected area. $\overline{Nu}$ based on the projected area will reflect the effect of the variation in the surface area as well as that of the disturbances in the flow due to the blocks on the heat transfer. But $\overline{Nu}$ based on the total area will reflect the effect of the flow disturbances (mixing) only. The latter is therefore used in determining the effects of the disturbances in the flow on the heat transfer. Once the flow disturbance effect is determined, the former is used in the evaluation of the effect of surface area increase (surface extension). An error analysis carried out according to a method given in Holman (1989) indicated that the uncertainty involved in experimental $\overline{Nu}$ measurements could be up to $\pm 9.5\%$.

Pressure drops over the test section in the channel can be represented in terms of the friction factor, which may be expressed as

$$f = \frac{\Delta P}{(L_{\text{t}}/D_{\text{e}})(\rho u^2/2)}, \tag{7}$$

where ρ is the density of the air, L_{t} the length of test section, and ΔP the pressure drop over the test section. An error analysis, using the same method as in the case of $\overline{Nu}$, indicated that the uncertainty involved in experimental f measurements could be up to $\pm 18.8\%$. The physical properties of the air were evaluated at $0.5 \times (\overline{T}_{\text{out}} + \overline{T}_{\text{in}})$.

4. Result and discussion

4.1. Heat transfer

In order to have a basis for the evaluation of the effects of the blocks, some experiments were carried out without any blocks attached to the plate, which will be called "smooth surface" hereafter. Using the data obtained from these tests, the average Nusselt number for the smooth surface ($\overline{Nu}_{\text{s}}$) was correlated as function of Re and Pr. The resultant equation was

$$\overline{Nu}_{\text{s}} = 0.0919\,Re^{0.706}\,Pr^{1/3} \quad 6670 \leqslant Re \leqslant 40\,000 \tag{8}$$

with a least-squares error of 0.63%.

If the Nusselt number for the surface with blocks ($\overline{Nu}$) calculated on the basis of the projected area of the test surface is normalised by $\overline{Nu}_{\text{s}}$, it will reflect the total effect of the blocks (surface extension as well as mixing) on the heat-transfer enhancement. In order to be able to infer the effect of the perforations, in what follows, $\overline{Nu}/\overline{Nu}_{\text{s}}$ for the surfaces with the perforated blocks will be presented together with those of the surfaces with the solid blocks. $\overline{Nu}_{\text{s}}$ is calculated by using Eq. (8) for the same experimental conditions as that of $\overline{Nu}$.

Results from the perforated blocks showed that as the degree of the perforation increased the heat-transfer enhancement capability of the blocks also increased. A typical variation in the heat transfer with Re for varying degree of the perforated open-area ratio ($\phi = 0.05$, 0.10 and 0.15) is shown in Fig. 2. S_x/D_{e}, D, and θ were fixed at values of 0.713, 4.5 mm and 30°, respectively. It should be noted here that the different levels of ϕ have been obtained by changing the number of the perforations (N) only and keeping the values of the rest of the

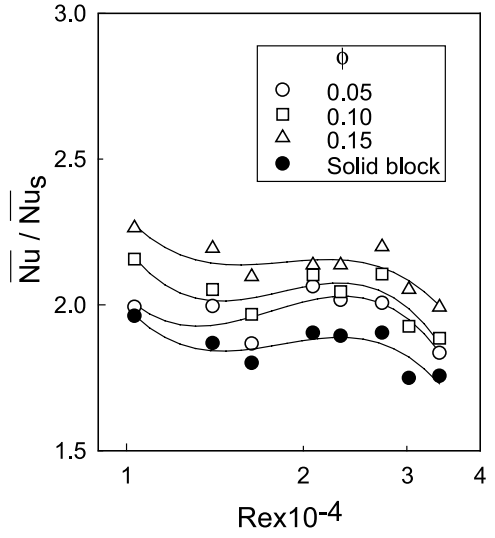

Fig. 2. Variation of $\overline{Nu}/\overline{Nu}_s$ with Re for various ϕ (N). $H/C = 0.454$, $S_x/D_e = 0.713$, $N_b = 4$, for perforated blocks only $D = 4.5$ mm, $\theta = 30°$.

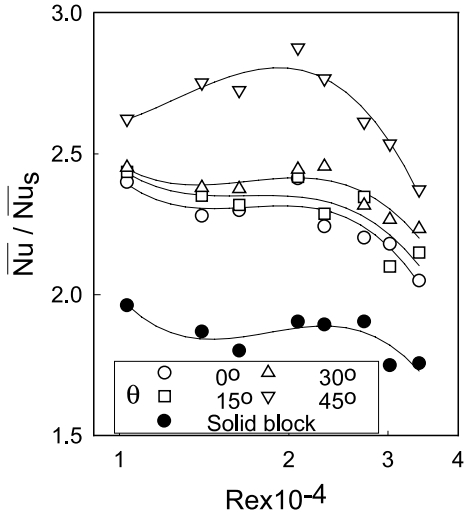

Fig. 3. Variation $\overline{Nu}/\overline{Nu}_s$ with Re for various θ. $H/C = 0.454$, $S_x/D_e = 0.713$, $N_b = 4$, for perforated blocks only $D = 8$ mm, $\phi = 0.1$ and $N = 3$.

parameters constant. The effect of ϕ can therefore be interpreted as the effect of N. The values of N corresponding to ϕ levels of 0.05, 0.10 and 0.15 are 3, 6, and 9, respectively. It is seen from this figure that $\overline{Nu}/\overline{Nu}_s$ increases with increasing ϕ. As mentioned above our earlier work (Sara et al., 2001) as well as that of Hwang and Liou (1994, 1995a) showed that solid blocks lead to flow separation from the surface and thus "dead" flow zones form in the immediate wake of the blocks. These dead flow zones are normally referred as separation bubbles (Liou et al., 1998). Above a critical degree of perforation, multiple jet-like flows due to the perforation will not only generate a mixing in the wake of the blocks, where otherwise separation bubbles exist, but also cause the flow to have better contact with the surface of the plate with increasing ϕ (i.e., increasing the number of perforations, N, therefore the number of jet-like flows). Thus, the heat transfer increases due to the improved flow conditions as ϕ increases. This clearly indicates that in the case of surfaces with attachments, whenever possible, the attachments must be designed in such a way that they will provide high flow permeability for a better heat-transfer performance. The behaviour of the data shown in Fig. 2 may also be useful in inferring the effect of the blocks on the flow pattern. Similar behaviour displayed by all the curves indicates that the flow pattern is similarly influenced with increasing Re for both the perforated and solid blocks. But the fact that the data lines are not straight and parallel to the Re axis means that flow pattern over the blocked surfaces is influenced by Re differently than that over the smooth surface.

The effect of the perforation inclination angle (θ) on the heat transfer is shown in Fig. 3 as a function of Re. S_x/D_e, D, N, and ϕ were fixed at values, 0.713, 8 mm, 3, and 0.1, respectively. It can be seen from this figure that both solid and perforated blocks cause substantial enhancement in the heat transfer with respect to that from the smooth surface. Due to the multiple jet-like flows, the enhancement in heat transfer with the perforated blocks is higher than that with the solid blocks for all the values of θ studied. The effect of inclined perforations on the heat transfer does not vary significantly with θ until $\theta \geqslant 30°$. As the inclination of the perforations increases further, the heat-transfer performance of the system gets better and for $\theta = 45°$ the heat transfer is enhanced up to approximately threefold with respect to that of the smooth surface. Studies on single jet flows impinging on flat surfaces (Pekdemir, 1994) report that for an impingement angle (i.e., inclination angle, θ) of 45°, the average heat transfer from the surface is approximately 20% less than for the case of normal impingement, whereas it may be as much as 65% less when the impingement angle is 20°. It is anticipated that if the impingement angle approaches $\theta = 0°$ (i.e., no inclination, straight perforations), the reduction in the heat transfer with respect to that from a normal impingement case may be over 90%. The situation in the case of the multiple impinging jets will be different due to the interaction between neighbouring jets following their impact on the surface which generally influences the heat-transfer capacity of each individual jet in a negative way. The importance of the negative effect will be a strong function of the spatial arrangement of the multiple jets. Considering the multiple jet-like flows through the perforations in the present work, it is anticipated that the perforations with an inclination angle of $\theta = 45°$ may be able to yield a heat-transfer rate similar to that of multiple normal impinging jets and much more than that of straight perforation. In fact, Fig. 3 indicates that, in the most favourable conditions, the heat-transfer performance for the perforations with 45° is approximately 30% and 60% better than that of straight perforations ($\theta = 0°$) and that of solid blocks, respectively. This is a significant improvement in the heat-transfer rate. Thus we recommend that, for better heat-transfer performance from surfaces with the perforated blocks, the perforations should be designed in such a way that air is forced through the perforations towards the heat-transfer surface as directly as possible.

The declining pattern of the curves with increasing Re, especially beyond 25 000, indicates that, although the blocks cause heat-transfer enhancement at any given Re, increasing Re influences the flow pattern over the surface with blocks less favourably than over the smooth surface. A similar behaviour for perforated blocks for $\theta \leqslant 30°$ with that of the solid blocks implies that the changes in the flow conditions with increasing Re is similar. For $\theta > 30°$, however, increasing Re influences the flow conditions differently. For example, in contrast to the other cases, when $\theta = 45°$, heat transfer increases with increasing Re up to $Re \approx 20\,000$ where it reaches a peak value and further increases in Re yield a steep drop in the heat

transfer. As enhancement in the heat transfer is due to the jet-like flows, this behaviour can be explained by the effects of the interaction between neighbouring jet-like flows on the flow following their impact on the surface. Jet-like flows from the perforations, as mentioned earlier, will be directed towards the heated surface more with increasing θ and the flow conditions will be approaching that of a normal impinging jet flow. When a jet flow impacts normally onto a surface, an accelerated flow (wall jet) will develop and spread out from the impact point. A study of the mass and fluid flow characteristics of multiple normal impinging jet flows (Pekdemir, 1994) for a jet flow Reynolds number of 1.9×10^5 reports that the wall jets arising from each impinging jet collide with those of neighbouring jets causing the flow to separate from the surface. The extent of the separated flow will be a function of the spatial distances between the jets and the jet Reynolds number (for fixed values of the other geometrical parameters) and significant deterioration in the heat transfer from the surface may result. In the present case (the Reynolds number for the jet-like flows through the perforations were not measured but will be proportional to the bulk flow mean Reynolds number, *Re*), if the perforations (i.e., multiple nozzles) are widely spaced and the jet Reynolds number is sufficiently small, collisions between the wall jet flows may not be intense enough to cause flow separation from the surface. Thus, initially, an increase in heat transfer occurs with increasing *Re* up to around 20 000 where heat transfer reaches a maximum. As *Re* increases further the "negative" effect of the wall-jet flow collisions rapidly increases which causes a drop in the heat transfer from the surface.

It was observed that $\overline{Nu}/\overline{Nu}_s$ increased as the perforation diameter (D) increased. Typical variations of $\overline{Nu}/\overline{Nu}_s$ with *Re* are shown in Fig. 4 for varying ϕ, D and N (S_x/D_e, N_b, and θ were fixed at values of 0.713, 4, and 30°, respectively). A given degree of perforation (i.e., ϕ) can be obtained by changing either D or N while keeping the other constant or changing both D and N simultaneously. For a number of blocks (i.e., $N_b = 4$) with the same ϕ, Fig. 4 shows that when an increment in ϕ (from 0.05 to 0.10) is realised by increasing D (from 4.5 mm to 8 mm) while keeping N constant (at 3), the enhancement in the heat transfer is significantly greater than if the same increment in ϕ is obtained by increasing N (from 3 to 6) while keeping D constant (at 4.5 mm). Moreover, Fig. 4 shows that, despite a decrease in N from 6 to 3, if D is increased from 4.5 mm to 8 mm, the heat transfer is also enhanced significantly, even though ϕ remains unchanged (i.e., at 0.1). This indicates that, for a given number of blocks with each having the same fixed level of ϕ, D plays a more important role in the enhancement of the heat transfer than N and that it may be more advantageous to obtain higher degree of perforations by increasing the diameter of perforations rather than the number. The reason for this may be explained by the effect of increasing the nozzle diameter on (1) the variation in the transport characteristics of multiple round jets and (2) the variation in the sum of the cross-sectional areas of the perforations in a single block (indicated as area in the legend in Fig. 4) which will be one of the most important factors in determining the proportion of the flow through the perforations (and thus the intensity of the jet-like flows). It has been reported by Pekdemir (1994) that, for round jets, the jet nozzle diameter is one of the most important parameters determining their transport characteristics. For a given nozzle the expansion of the jet flow in the radial direction and also the velocity and turbulence intensity distribution in any cross-section of the flow along the bulk flow (axial) direction will be mainly governed by the nozzle diameter. For a given axial distance, the higher the nozzle diameter the higher the radial expansion will be. Thus, in the case of blocks with multiple perforations, the radial expansion of each of the jet-like flows through the perforations will be larger for larger D. If D is large enough, the radial expansions will lead neighbouring jet-like flows to interact with each other. This will promote a higher degree of flow mixing and help to eliminate the separated flow zones downstream of each block thus yielding a higher heat-transfer enhancement. For a given block, as seen in Fig. 4, the perforations for $D = 8$ mm yield a higher total area available to the jet-like flows (151 mm^2) when N is small ($=3$) than that of the perforations of smaller D ($=4.5$ mm) when N is large ($=6$), 96 mm^2. If D and N are both small (i.e., 4.5 mm and 3, respectively), the area is even smaller (48 mm^2). For a given *Re* and fixed levels of the other geometrical parameters, the higher the total area available to the jet-like flows the higher their flow rates will be. As the enhancement in heat transfer is brought by the jet-like flows, the higher flow rates (i.e., higher Ds) will lead to higher heat-transfer enhancement.

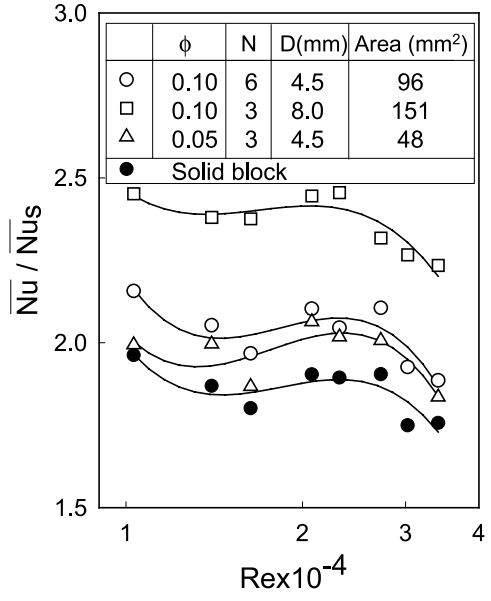

Fig. 4. Variation of $\overline{Nu}/\overline{Nu}_s$ with *Re* for various D, N and ϕ. $H/C = 0.454$, $S_x/D_e = 0.713$, $N_b = 4$, for perforated blocks only $\theta = 30°$.

The effect of S_x/D_e on $\overline{Nu}/\overline{Nu}_s$ is shown in Fig. 5 as a function of *Re* for fixed values of θ, ϕ, N, and D at 30°, 0.10, 6, and 4.5 mm, respectively. The number of blocks, N_b, corresponding to studied different S_x/D_e values of 1.407, 1.116, 0.713, and 0.309 were 2, 3, 4, and 7, respectively. For the solid blocks, Fig. 5(a) shows that the enhancement of the heat transfer is almost identical for three different spacing. For the perforated blocks, on the other hand, $\overline{Nu}/\overline{Nu}_s$ increases only slightly with decreasing S_x/D_e for $S_x/D_e \geqslant 0.713$, but for $S_x/D_e = 0.309$, $\overline{Nu}/\overline{Nu}_s$ becomes significantly higher than the rest of the cases. In all cases the effect of the block spacing (i.e., the number of blocks) on the heat-transfer enhancement is higher for the perforated blocks than for the solid blocks because of the improved flow conditions due to the presence of the perforations as shown and discussed above (Figs. 2–4). Figs. 5(b)–(d) indicate that the perforated blocks are able to improve the heat transfer more significantly as the blocks are spaced more densely (larger number of blocks). This improvement in heat transfer is due to the increasing number of jet-like flows (in the order of 12, 18, 24, and 48) as the number of the blocks increases (in the order of 2, 3, 4, and 7). This result agrees with the findings of Hwang and Liou (1994) obtained with straight perforations. Consequently, for better

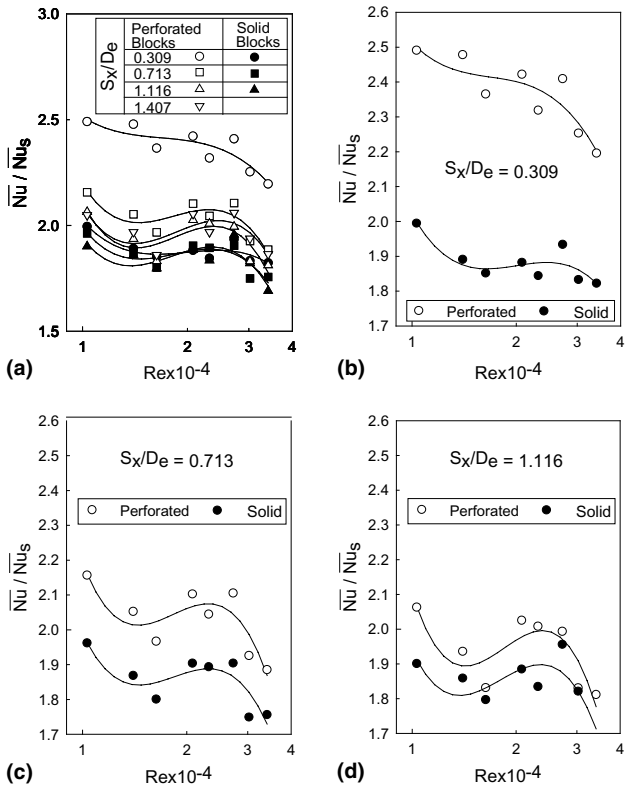

Fig. 5. Variation $\overline{Nu}/\overline{Nu}_s$ with Re for (a) various $S_x/D_e(N_b)$, (b) $S_x/D_e = 0.309$ ($N_b = 7$), (c) $S_x/D_e = 0.713$ ($N_b = 4$), and (d) $S_x/D_e = 1.116$ ($N_b = 3$). $H/C = 0.454$, for perforated blocks only $D = 4.5$ mm, $\theta = 0$, $\phi = 0.1$ and $N = 6$.

heat-transfer performances, it is important to space the blocks an optimum distance from each other.

Fig. 5 shows that $\overline{Nu}/\overline{Nu}_s$, in general, decreases with increasing Re and displays nearly the same trend with Re for the solid and perforated blocks. It should be remembered here that the curves in Fig. 5 represent heat-transfer performance of the surfaces with blocks in comparison to that of the surface without blocks. For a given Re, although the perforations can eliminate the recirculating flows in front of and behind the solid blocks (thus yielding a higher enhancement in the heat transfer), the variation in the overall flow conditions over the surface may be influenced in a similar manner with varying Re for the solid and the perforated blocks. This is thought to be the reason for the same trend with Re for the solid and the perforated blocks. This conclusion on the flow conditions inferred from heat-transfer measurements needs to be confirmed by flow measurements which will be the subject of our forthcoming research.

The parameters used to describe the convective heat transfer in the present experiments have led to the following correlation equation:

$$\overline{Nu}/\overline{Nu}_s = 19.586\,Re^{-0.186}(S_x/D_e)^{-0.10} \times (D/D_e)^{0.05}(\phi)^{0.10}(1/\mathrm{Cos}\theta)^{0.17}. \quad (9)$$

This equation is plotted in Fig. 6 together with the experimental data used in its production. The indices of e and c in the axis titles (i.e., Nusselt number) denote experimental and calculated, respectively. The least-squares errors for this equation is 5.33%. It must be noted that the above equation is valid for $6670 \leqslant Re \leqslant 40\,000$, $0.309 \leqslant S_x/D_e \leqslant 1.40$, $0.05 \leqslant \phi \leqslant 0.15$, $2.5 \leqslant D \leqslant 8$, $0° \leqslant \theta \leqslant 45°$. This equation implies that enhancement in the heat-transfer rate increases with increasing D/D_e, ϕ and θ but decreasing S_x/D_e and Re. The magnitude of the powers to each parameter in the equation may be taken as an indication of the order of their influence on the heat-transfer enhancement. The perforation inclination angle, θ, is seen to have second highest influence after the most influential parameter, Re. This once again indicates the importance of θ in the heat-transfer enhancement. From the results presented in the above sections it is inferred that the heat-transfer enhancement effect of each parameter investigated is not independent from those of the rest. There appears to be interactions between them and it may not be an easy task to determine their optimum values within their given ranges. Eq. (9) provides a useful tool to predict not only enhancement in the heat-transfer rate with a given block geometry and flow conditions but also the value of any single parameter for a given heat-transfer enhancement when the rest of the parameters are fixed at given values. Thus it may also be useful in determining optimum values of the parameters investigated within a given range through an optimisation analysis. This will also be the subject of forthcoming studies.

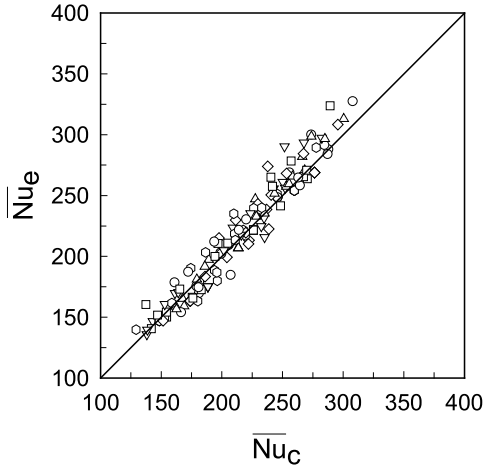

Fig. 6. Correlation of the heat transfer as function of the flow and geometrical parameters and its fitness to the experimental data. Valid for $6670 \leqslant Re \leqslant 40\,000$, $0.309 \leqslant S_x/D_e \leqslant 1.116$, $0.05 \leqslant \phi \leqslant 0.15$, $2.5 \leqslant D \leqslant 8$, $0° \leqslant \theta \leqslant 45°$.

4.2. Pressure drop

The pressure drops corresponding to the heat-transfer enhancement due to the blocks over the test section in the channel were measured under heated flow conditions. These measurements were converted to friction factor, f, using Eq. (7). The results indicated that the perforation inclination angle, within the range investigated ($\theta = 0°$, 15°, 30°, and 45°), had no detectable influence on the pressure drop. A typical example of the dependence of f on Re as a function of the number of blocks (spacing) for both the solid and perforated blocks is shown in Fig. 7. The open symbols represent the results for the perforated blocks for $\theta = 30°$, $\phi = 0.10$ and $D = 4.5$ mm at different block spacings shown in the legend. The results for solid blocks under the same flow conditions and for the same spacings are represented by solid symbols. Also given in this figure is the Blasius equation curve representing the pressure drop over a smooth surface for the same base plate dimensions. It is seen from the figure that f decreases with increasing Re. As the resistance to the flow will be smaller due

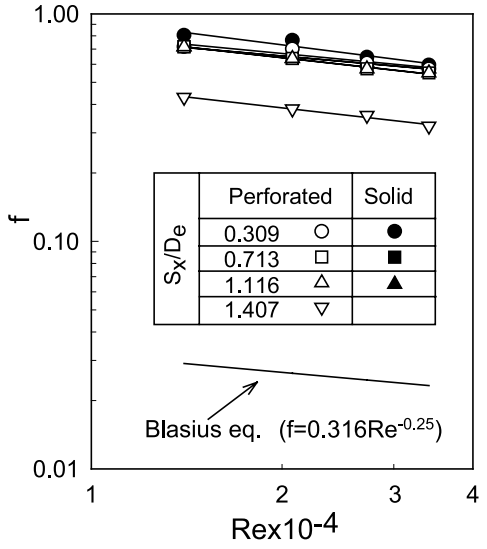

Fig. 7. Variation of f with Re for various $S_x/D_e(N_b)$. $H/C = 0.454$, for perforated blocks only $D = 4.5$ mm, $\theta = 30°$, $\phi = 0.1$ and $N = 6$.

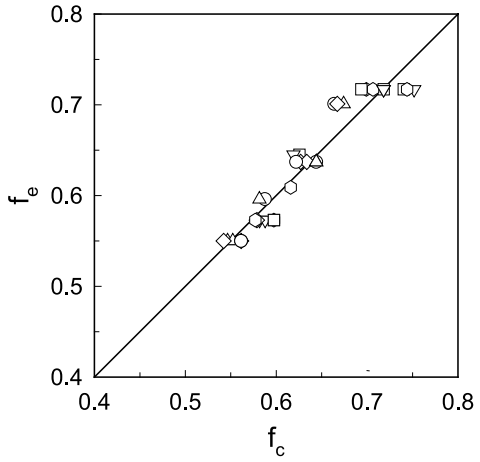

Fig. 8. Correlation of the friction factor as function of the flow and geometrical parameters and its fitness to the experimental data. Valid for $6670 \leqslant Re \leqslant 40\,000$, $0.309 \leqslant S_x/D_e \leqslant 1.116$, $0.05 \leqslant \phi \leqslant 0.15$, $2.5 \leqslant D \leqslant 8$, $0° \leqslant \theta \leqslant 45°$.

to the perforation, f is lower for the perforated blocks than for solid blocks. For solid blocks, f remains almost constant with increasing block spacing (i.e., decreasing number of blocks) while for perforated blocks it remains almost unchanged for only $S_x/D_e \leqslant 1.116$. This suggests the presence of a limit on the value of spacing (i.e., S_x/D_e) below which f is not influenced by the number of blocks. Further increase in S_x/D_e from 1.116 to 1.407, in the perforated block case, leads to a substantial decrease in f. This is because of the lesser cross-sectional blockage areas with increasing S_x/D_e (i.e., decreasing number of blocks). However, both the perforated and solid blocks cause a considerable increase in f with respect to the smooth surface. This clearly shows why the heat-transfer enhancement capacities of the surface attachments must always be considered in conjunction with the associated increases in the pressure drop they may be caused in the flow. Using the experimental results, the following correlation for f as a function of the flow and the geometrical parameters is proposed:

$$f = 7.074\,Re^{-0.277}(\phi)^{-0.066} \times (S_x/D_e)^{-0.036}(D/D_e)^{-0.060}. \quad (10)$$

As the inclination angle, θ, did not seem to have any detectable effect on the friction factor, it was not included in the correlation equation. The f values from Eq. (10) is plotted in Fig. 8 against experimentally measured f which were used in the production of this equation. It is seen that the equation fits reasonably well to the data with the least-squares errors of 2.44%. This equation is valid only for $6670 \leqslant Re \leqslant 40\,000$, $0.309 \leqslant S_x/D_e \leqslant 1.116$, $0.05 \leqslant \phi \leqslant 0.15$, $2.5 \leqslant D \leqslant 8$, $0° \leqslant \theta \leqslant 45°$. The exponents of the parameters in the equation indicate that increases in each of the parameters will lead to decreases in f. The flow rate (i.e., Re) seems to be most influential parameter as in the case of heat-transfer enhancement.

4.3. Thermal performance

As expected, the pressure drop measurements presented above showed that the enhancement in the heat-transfer rate is accompanied by an increase in the pressure drop. Thus, for the purpose of practical application, a thermal performance analysis is necessary. One performance evaluation criterion is the comparison of the heat-transfer coefficient for constant pumping power to overcome the resistance to the flow over the test section for the channel with extended (or roughened) surface with that for the smooth surface. The pumping power is proportional to $f^{1/3}Re$ and the relationship between the blocked and smooth channel for the same pumping power is expressed by $fRe^3 = f_sRe_s^3$ (Hwang and Liou, 1995b). Here $f$and Re are the values for the blocked channel, f_s and Re_s are those for the smooth channel. In the present study, the ratios of $\overline{Nu}/\overline{Nu}_s^*$ are plotted against Re_s. $\overline{Nu}_s^*$ is the average Nusselt number for the smooth channel with Re_s at which the pumping power is the same as that occurring in the blocked channel. The evaluation of $\overline{Nu}_s^*$ is given in detail by Liou and Hwang (1992).

Fig. 9(a) shows the effect of θ on the thermal performance of the perforated blocks for fixed values of S_x/D_e, D, and ϕ at of 0.713, 8 mm and 0.1, respectively, in comparison to the thermal performance of the solid blocks under the same conditions. Also given in this figure are some previous results reported in the related literature for different rib geometries. The experimental conditions for the literature data were as follows. Liou et al. (1995): detached ribs, $P/H = 10$, $K/H = 1$ (P: spacing between the back surfaces of two consecutive blocks, H: height of the blocks, K: detachment spacing between the lower surface of the block and the heat-transfer surface); Hwang and Liou (1994): permeable ribs, $P/H = 10$, $H/D_e = 0.162$, $\phi = 0.22$ ($\phi = (n\pi\varphi^2)/(2ZH)$, Z: the half-width of channel, ϕ: radius of the perforation and n: the number of perforations in a rib). This figure shows that $\overline{Nu}/\overline{Nu}_s^*$ increases with increasing θ. $\overline{Nu}/\overline{Nu}_s^*$ is larger than unity for all θ values being investigated indicating that θ has a favourable effect on the overall energy performance of the system. There appears to be a net energy gain (as much as 40% in comparison to that from the smooth surface) due to the perforated blocks while, for the solid blocks, it is seen from the figure that $\overline{Nu}/\overline{Nu}_s^*$ is, except at very low Re, less than unity. This indicates that solid blocks lead to a net energy loss (as much as 20% in comparison to that from the smooth surface) from the system. In contrast, it is seen from the figure that the perforated blocks may lead to an energy gain of approximately 77% with respect to the performance of solid blocks. This is because of the higher heat-transfer enhancement and the lower pressure drop in the case of the perforated blocks.

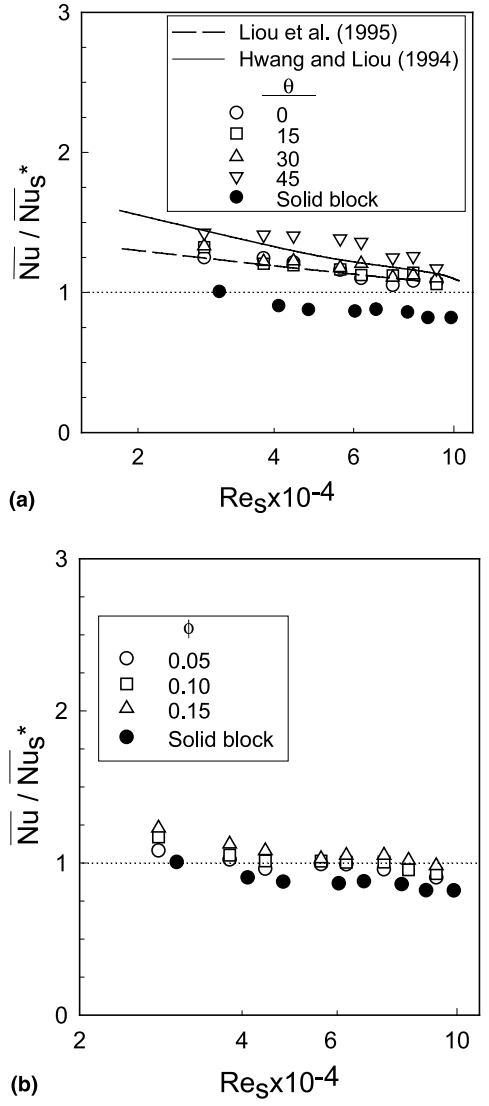

Fig. 9. Heat-transfer improvement performance of the perforated blocks in comparison to that of the solid blocks under a constant pumping power constraint. (a) For various θ, $\phi = 0.1$, $S_x/D_e = 0.713$ ($N_b = 4$), $D = 8$ mm and $N = 3$ and a comparison with some data from the literature, (b) for various $\phi(N)$, $\theta = 30°$, $S_x/D_e = 0.713$ ($N_b = 4$), $D = 4.5$ mm.

Fig. 9(b) shows the effect of ϕ for fixed values of S_x/D_e, D, and θ at of 0.713, 4.5 mm and 30°, respectively. It is seen from the figure that $\overline{Nu}/\overline{Nu}_s^*$ remains almost constant with changing ϕ. The values of $\overline{Nu}/\overline{Nu}_s^*$ for the perforated blocks are not significantly higher than those for the solid blocks for this particular geometrical arrangement. This seems to be in contrast to the behaviour displayed in Fig. 9(a). It should be noted here that the perforation hole diameter, D, is 8 mm for the data in Fig. 9(a) whereas it is 4.5 mm for those in Fig. 9(b). This means that D for the data in Fig. 9(b) is 44% smaller than that in Fig. 9(a). That is why perforated blocks in Fig. 9(b) do not yield as much improvement in the overall energy performance as those in Fig. 9(a). This indicates, as also shown in Fig. 4, that perforations with larger diameter yield better heat-transfer rate performance. For a constant θ, increasing ϕ does not influence $\overline{Nu}/\overline{Nu}_s^*$ as much in comparison to its influence on $\overline{Nu}/\overline{Nu}_s$ (see Fig. 2). This implies that the enhancement in the heat transfer is accompanied with a pressure drop of similar magnitude of energy with increasing ϕ. It appears that the effect of each individual parameter is dependent on the other parameters.

Figs. 9(a) and (b) show that both the perforated and solid blocks give a higher thermal performance at lower Re. In terms of heat-transfer improvement, this means that the blocks are more effective at low Re.

5. Conclusions

Enhancement of the heat transfer from a flat surface in a rectangular channel flow by the attachment of perforated rectangular cross-sectional blocks has been investigated as function of the flow and geometrical parameters. Pressure drops corresponding to the heat-transfer enhancement have also been measured. Heat-transfer performance analysis have been carried out in relation to the pressure drops. The conclusions are summarised as follows:

- Perforations in the blocks enhances the heat transfer and the enhancement increases with increasing the degree of perforations. For a given number of blocks, with each having same number of perforations, the diameter plays a more important role in the enhancement of the heat transfer than the number of perforations does. Thus, it may be more advantageous to obtain higher degree of perforation by increasing the diameter of perforations rather than their numbers.
- Blocks with inclined perforations achieve better heat-transfer rates in comparison to that of the blocks with straight perforations. Depending on the inclination angle, perforated blocks may lead, respectively, to approximately 30% and 60% improvement in heat-transfer rate in comparison to that from blocks with straight perforations and that from solid blocks. Increases in the perforation inclination angle yield higher heat-transfer rates.
- More densely spaced blocks yield better heat transfer. The effect of the block spacing (i.e., the number of blocks) on the heat-transfer enhancement is higher for the perforated blocks than for the solid.
- Heat transfer from the smooth surface has been correlated as a function of the flow conditions. The resultant equation was

$$\overline{Nu}_s = 0.0919\,Re^{0.706}\,Pr^{1/3} \quad 6670 \leqslant Re \leqslant 40\,000.$$

- Heat transfer with perforated-block arrangements has also been correlated as a function of the flow and geometrical parameters. The resultant equation was

$$\overline{Nu}/\overline{Nu}_s = 19.586\,Re^{-0.186}(S_x/D_e)^{-0.10} \times (D/D_e)^{0.05}(\phi)^{0.10}(1/\mathrm{Cos}\theta)^{0.17},$$

$$6670 \leqslant Re \leqslant 40\,000, \quad 0.309 \leqslant S_x/D_e \leqslant 1.40,$$
$$0.05 \leqslant \phi \leqslant 0.15, \quad 2.5 \leqslant D \leqslant 8,$$
$$0° \leqslant \theta \leqslant 45°.$$

- Pressure drops in terms of friction factor due to the perforated blocks is smaller in comparison to those due to the solid blocks. The perforation angle does not induce any detectable changes in the friction factor. However, both the perforated and solid blocks cause a substantial increase in friction factor with respect to the smooth surface. Friction factor decreases with increasing Re for both the perforated and solid blocks.
- The friction factor has been correlated as a function of the flow and geometrical parameters. The resultant equation was

$$f = 7.074\,Re^{-0.277}(\phi)^{-0.066} \times (S_x/D_e)^{-0.036}(D/D_e)^{-0.060}$$

$6670 \leqslant Re \leqslant 40\,000$, $0.309 \leqslant S_x/D_e \leqslant 1.116$,
$0.05 \leqslant \phi \leqslant 0.15$, $2.5 \leqslant D \leqslant 8$,
$0^\circ \leqslant \theta \leqslant 45^\circ$.

- In comparison to the energy performance of the smooth surface, the surfaces with perforated blocks yield a net energy gain up to 40%, whereas those with solid blocks lead to a net energy loss up to 20% from the system. The perforated blocks may lead to an energy gain of approximately 77% with respect to the performance of solid blocks because of the higher heat-transfer enhancement and the lower pressure drop in the case of the perforated blocks.
- For the perforated blocks, the higher the perforation diameter, perforated area open-area ratio, and the inclination of perforation holes, the better the overall energy performance.

References

Babus'Haq, R.F., Probert, S.D., Taylor, C.R., 1993. Heat transfer effectiveness of shrouded rectangular-fin arrays. Appl. Energy 46, 99–112.

Bergles, A.E., Webb, R.L., 1985. A guide to the literature on convective heat transfer augmentation. Adv. Enhanced Heat Transfer HTD43, 81–89.

Goldstein, R.J., Jabbari, M.Y., Chen, S.B., 1994. Convective mass transfer and pressure loss characteristics of staggered short pin-fin arrays. J. Heat Mass Transfer 37, 149–160.

Han, J.C., 1988. Heat transfer and friction characteristics in rectangular channels with rib turbulators. J. Heat Transfer 110, 321–328.

Holman, J.P., 1989. Experimental Methods for Engineers, fifth ed. McGraw-Hill, New York, pp. 41–49.

Hong, Y.J., Hsieh, S.S., 1993. Heat transfer and friction factor measurements in duct with staggered and in-line ribs. J. Heat Transfer 115, 58–65.

Hwang, J.J., 1998. Heat transfer-friction characteristics comparison in rectangular ducts with slit and solid ribs mounted on one wall. J. Heat Transfer 120, 709–716.

Hwang, J.J., Liou, T.M., 1994. Augmented heat transfer in a rectangular channel with permeable ribs mounted on the wall. J. Heat Transfer 116, 912–920.

Hwang, J.J., Liou, T.M., 1995a. Effect of permeable ribs on heat transfer and friction in a rectangular channel. J. Heat Transfer 117, 265–271.

Hwang, J.J., Liou, T.M., 1995b. Heat transfer and friction in a low-aspect-ratio rectangular channel with staggered perforated ribs on two opposite walls. J. Heat Transfer 117, 843–850.

Ichimaya, K., Katayama, M., Miyazawa, T., Kondoh, H., 1991. Experimental study on effects of a single porous-type roughness element in a parallel plate duct. Exp. Heat Transfer 4, 319–330.

Incropera, F.P., Dewitt, D.P., 1996. Fundamentals of Heat and Mass Transfer, fourth ed. Wiley, New York, pp. 496–499.

Jurban, B.A., Hamdan, M.A., Abdualh, R.M., 1993. Enhanced heat transfer, missing pin, and optimisation for cylindrical pin fin arrays. J. Heat Transfer 115, 576–583.

Lau, S.C., McMillin, R.D., Han, J.C., 1991. Turbulent heat transfer and friction in a square channel with discrete rib turbulators. ASME J. Turbomach. 113, 360–366.

Ledezma, D., Morgan, A.M., Bejan, A., 1996. Optimal spacing between pin fins with impinging flow. J. Heat Transfer 118, 570–577.

Liou, T.M., Chen, S.H., 1998. Turbulent heat and fluid flow in a passage disturbed by detached perforated ribs of different heights. J. Heat Mass Transfer 41, 1795–1806.

Liou, T.M., Hwang, J.J., 1992. Turbulent heat transfer augmentation and friction in periodic fully developed channel flows. J. Heat Transfer 114, 56–64.

Liou, T.M., Hwang, J.J., 1992. Developing heat transfer augmentation and friction in a rectangular ribbed duct with flow separation at inlet. J. Heat Transfer 114, 565–573.

Liou, T.M., Hwang, J.J., 1993. Effect ridge shapes on turbulent heat transfer and friction in a rectangular channel. J. Heat Mass Transfer 36, 931–940.

Liou, T.M., Kao, C.W., Chen, S.H., 1998. Flowfield investigation of the effect of rib open area ratio in a rectangular duct. J. Fluids Eng. 120, 504–512.

Liou, T.M., Wang, W.B., Chang, Y.J., 1995. Holographic interferometry study of spatially periodic heat transfer in a channel with ribs detached from one wall. J. Heat Transfer 117, 32–39.

Molki, M., Faghri, M., Ozbay, O., 1995. A correlation for heat transfer and wake effect in the entrance region of an in-line array of rectangular blocks simulating electronic components. J. Heat Transfer 117, 40–46.

Molki, M., Mostoufizadeh, A.R., 1989. Turbulent heat transfer in rectangular ducts with repeated-baffle blockages. J. Heat Mass Transfer 32, 1491–1499.

Naik, S., Probert, S.D., Shilston, M.J., 1987. Forced-convective steady-state heat transfer from shrouded vertical fin arrays aligned parallel to an undisturbed air-stream. Appl. Energy 26, 137–158.

Pekdemir, T., 1994. Convective mass transfer from stationary and rotating cylinders in a jet flow. Ph.D. thesis, University of Exeter, Exeter, UK.

Reay, D.A., 1991. Heat transfer enhancement – a review of techniques and their possible impact on energy efficiency in the UK. Heat Recovery Syst. CHP 11, 1–40.

Sara, O.N., 1998. Effect of prismatic perforated turbulators on heat transfer, Ph.D. Thesis, Atatürk University, Erzurum, Turkey (in Turkish).

Sara, O.N., Pekdemir, T., Yapici, S., Yilmaz, M., 2001. Enhancement of heat transfer from a flat surface in a channel flow by attachment of rectangular blocks. Int. J. Energy Res. 25, 563–576.

Tahat, M.A., Babus'Haq, R.F., Probert, S.D., 1994. Forced steady-state convections from pin-fin arrays. Appl. Energy 48, 335–351.

Tanasawa, I., Nishio, S., Takano, K., Tado, M., 1983. Enhancement of forced convection heat transfer in rectangular channel using turbulence promoters. In: Proceedings of ASME-JSME Thermal Engineering Joint Conference, pp. 395–402.

Yamada, H., Osaka, H., 1992. Flow around a permeable rectangular plate standing on the flat wall, 2nd report, effects of the aspect and open area ratios. Trans. JSME 56, 120–128.

Zhang, Y.M., Gu, W.Z., Han, J.C., 1994. Heat transfer and friction in rectangular channels with ribbed or ribbed-grooved walls. J. Heat Transfer 116, 58–65.